TI Designs: TIDA-01187
LIDAR-Pulsed Time-of-Flight Reference Design Using High-Speed Data Converters

Description

A variety of applications utilize time-of-flight (ToF) optical methods for measuring distance with high-precision, such as laser safety scanners, range finders, drones, guidance, and autonomous driving systems. This reference design details the advantages of a high-speed data-converter based solution, including target identification, relaxed sample rate requirements, and a simplified signal chain. The design also addresses optics, driver and receiver front-end circuitry, analog-to-digital converters (ADCs), digital-to-analog converter (DAC), and signal processing.

Resources

TIDA-01187	Design Folder
ADC3244	Product Folder
DAC5682Z	Product Folder
OPA695	Product Folder
OPA857	Product Folder
THS4541	Product Folder
CDCM7005	Product Folder

TI E2E™ Community — ASK Our E2E Experts

Features

- Measurement Range up to 9 m or Greater With Additional Optics and Laser Power
- Range Measurement Mean Error of < ±6 mm and Standard Deviation of < 3 cm
- 5.75-W Pulsed 905-nm Near Infrared Laser Diode and Driver With < 1-mW Average Output Power
- Near Infrared PIN Photodiode High-Speed Transimpedance Amp Front End
- Laser Collimation and Photo Receiver Focusing Optics
- Includes 14-Bit, 125-MSPS ADCs and 16-Bit, 500-MSPS DAC High-Speed Amplifiers and Clocking
- Pulsed ToF Measurement Method With DFT-based Range Estimation
- Automotive Grade Versions Available for Select Devices

Applications

- Architectural Surveying Equipment
- Automotive Scanning LIDAR
- Drones
- Gas Analysis
- Laser Range Finders (LIDAR)
- Laser Safety Scanners
- Retinal Imaging
- Robotics

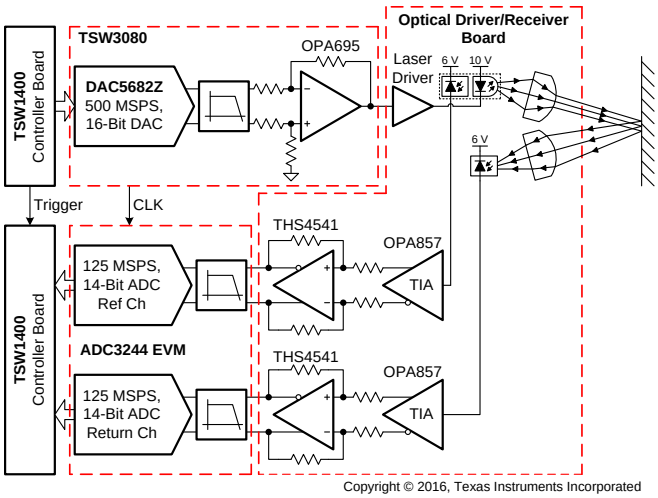

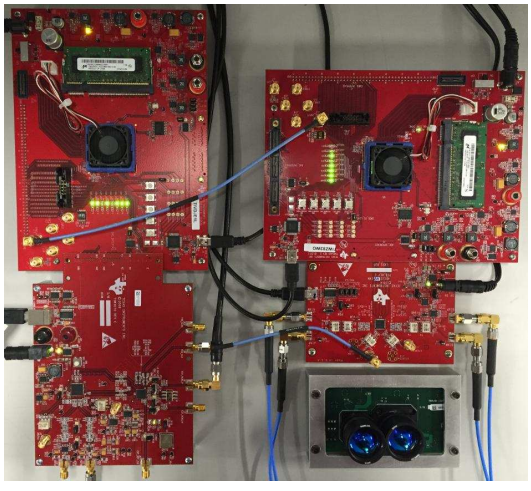

1 System Description

The coherent nature of light emitted from a laser makes it especially useful in the measurement of distance because it can be easily collimated into a narrow beam with minimal divergence. The constant speed of light at approximately 3×10^8 m/s can be used to estimate distance by measuring the time it takes for the emitted light of a laser to travel to the target and back. Small laser and photo diodes have made it possible to build compact and portable systems, which enable applications including laser safety scanners, drones, laser range finders and guidance systems.

1.1 Key System Specifications

Table 1. Key System Specifications

PARAMETER	SPECIFICATIONS	DETAILS
Range	1.5 m to 9 m	Section 3.5
Range measurement standard deviation	< 1 cm at 5 m, < 3 cm at 9 m	Section 3.5
Range measurement mean error	< ±6 mm	Section 3.5
Laser peak power	5.75 W	Section 2.3.6.3
Laser average power	< 1 mW	Section 2.3.6.3
Wavelength	905 nm	Section 3.3

2 System Overview

Figure 1 shows a simplified diagram of a laser-based distance measurement system. In this system, light emitted by the laser is first collimated by a lens to create a narrow beam, which then travels down range and after reflecting off the target returns back to be focused on the detector by a second lens. The laser driver and stimulus subsystem can be designed to apply pulsed or amplitude modulation (AM) waveforms. Some lasers are capable of frequency modulation (FM) (that is, modulation of the emitted wavelength), but they are beyond the scope of this design.

The optical detector is typically a PIN or avalanche photo diode, which produces a small current proportional the return signal. A very-low-noise transimpedance amplifier (TIA) is required to optimize the range of the system because the amplitude of the return signals decreases proportionally to the square of the distance. The amplified return signal is measured and processed to produce a range measurement. The optics used in this design are optimized for up to 9 m of distance. A longer range is possible through a choice of optics.

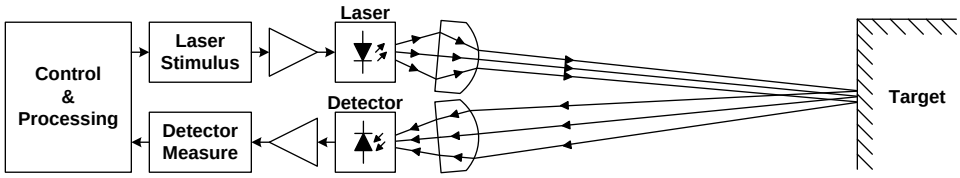

Figure 1. Simplified System Diagram

This design highlights the advantages of a high-speed ADC or DAC based signal chain for laser distance measurement systems. The guide also describes a pulsed ToF-based system using phase-shift based range estimation.

2.1 Block Diagram

This design comprises five circuit boards that work together to form a system for laser distance measurement.

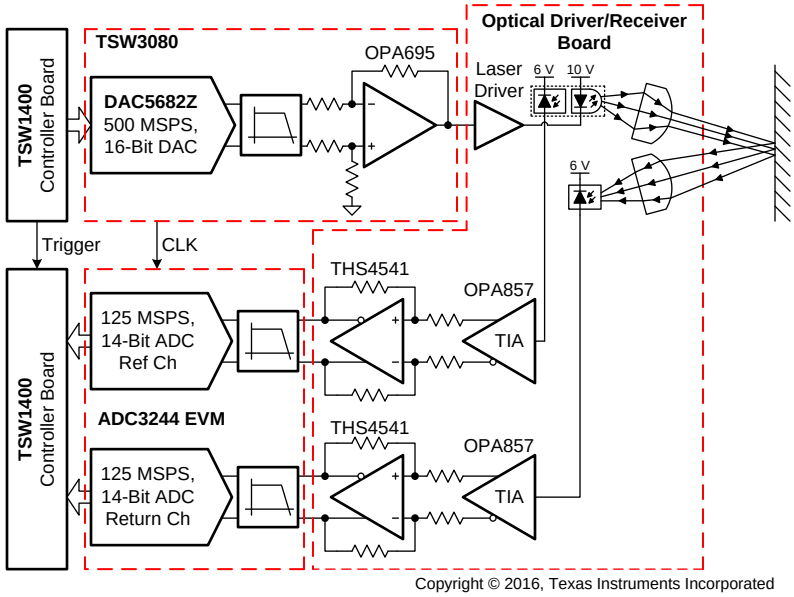

Figure 2. Block Diagram

2.1.1 Optical Driver and Receiver Board

This board contains the laser driver, near infrared (NIR) laser diode, laser collimating lens, receiver focusing lens, PIN receiver and reference photo diodes, and corresponding TIAs. Laser driver stimulus input from the DAC evaluation module (EVM) and TIA received output from the TIAs to the ADC EVM is provided through SMP coax connectors. The optics are off-the-shelf components available from Thorlabs.

2.1.2 TSW3080 Board

This board provides the laser driver stimulus and is based on the DAC5682Z 1-GSPS DAC and OPA695 high-speed operational amplifier (op amp). The DAC is operated at 500 MSPS with no interpolation. A divide-by-4 version of the DAC clock is connected to the ADC EVMs clock input so that the boards sample coherently with respect to each other. A RF signal generator is used to provide a 1-GHz clock for the system.

2.1.3 ADC3244 EVM

The EVM for the ADC3244 provides a dual-channel, 14-bit, 125-MSPS ADC used to capture input from both the reference TIA and return signal TIA. These inputs are bandwidth limited to 40 MHz by the boards low-pass filters.

2.1.4 TSW1400 Controller Board

Two TSW1400 controller boards are used in the system. The first board is used to drive the stimulus signal into the DAC while the other board captures the output of the reference and return signal channels. The triggering features of these boards are utilized to create a synchronized capture between the DAC and the ADC.

2.2 Highlighted Products

2.2.1 ADC3244

The ADC3244 is a high-linearity, ultra-low-power, dual-channel, 14-bit, 125-MSPS, ADC with a serial low-voltage differential signaling (LVDS) to reduce the number of interface lines. The serial LVDS interface is two-wire, where each ADC data are serialized and output over two LVDS pairs. An internal phase-locked loop (PLL) multiplies the incoming ADC sampling clock to derive the bit clock that is used to serialize the 14-bit output data from each channel. In addition to the serial data streams, the frame and bit clocks are also transmitted as LVDS outputs. The ADC3244 is available in a VQFN-48 package (7 mm × 7 mm).

2.2.2 DAC5682Z

The DAC5682Z is a dual-channel, 16-bit, 1-GSPS DAC with wideband LVDS data input, integrated 2×/4× interpolation filters, onboard clock multiplier, internal voltage reference and a wideband LVDS port with on-chip termination. Full-rate input data can be transferred to a single DAC channel, or ½-rate and ¼-rate input data can be interpolated by onboard 2×- or 4×-FIR filters. An on-chip delay lock loop (DLL) simplifies LVDS interfacing by providing skew control for the LVDS input data clock. The DAC5682Z is available in a QFN-64 package (9 mm × 9 mm).

2.2.3 OPA695

The OPA695 is a 1400-MHz bandwidth (gain = 2 V/V), current-feedback op amp that combines an exceptional 4300-V/µs slew rate and low input voltage noise. The device is available in SOIC-8, VSSOP-8, and SOT23-6 packages.

2.2.4 OPA857

The OPA857 is a wideband, fast overdrive recovery, fast-settling, ultra-low-noise TIA that targets photodiode monitoring applications. With selectable feedback resistance, the OPA857 simplifies the design of high-performance optical systems. Very-fast overload recovery time and internal input protection provide the best combination to protect the remainder of the signal chain from overdrive while minimizing recovery time. The two selectable transimpedance gain configurations allow the high dynamic range and flexibility required in modern TIA applications. The OPA857 is available in a VQFN (3 mm × 3 mm) package.

2.2.5 THS4541

The THS4541 is a low-power, voltage-feedback, fully differential amplifier (FDA) with an input common-mode range below the negative rail and rail-to-rail output. The device has a 1500-V/μs slew rate, a 500-MHz bandwidth (gain = 2 V/V) and is available in VQFN-16 (3 mm × 3 mm) and WQFN-10 (2 mm × 2 mm) packages.

2.2.6 CDCM7005

The CDCM7005 is a high-performance, low-phase-noise and low-skew clock synchronizer that synchronizes a VCXO or VCO frequency to one of the two reference clocks. The programmable pre-divider M and the feedback-dividers N and P give high flexibility to the frequency ratio of the reference clock to VCXO. The outputs are user definable to LVCMOS or LVPECL. This device is available in a 48-pin VQFN (7 mm x 7 mm) or a 64-pin BGA (8 mm x 8 mm).

2.3 System Design Theory

2.3.1 Pulsed ToF Method Overview

The most direct way to estimate distance using the system mentioned in the previous sections is to apply a short duration pulse to the laser and measure the time from when the pulse of light is emitted until it returns to the detector. ToF can be measured using a time-to-digital converter (TDC) or a high-speed ADC and the resulting distance can be calculated using the following Equation 1. The TDC operates like a high-speed stopwatch directly counting time between start and stop events, while the ADC measures the return signal at a regular interval, which is then processed to estimate time. As Equation 1 shows, because of the high speed of light, small amounts of time equate to substantial distances. For instance, ±1 ns of error in the measurement of time results in ±15 cm of distance estimation error. The range estimation performance of pulsed ToF measurement is therefore directly proportional to the ability of the system to measure small time intervals.

$$d = \frac{c \times t}{2} \quad (1)$$

where

- d is the distance in meters
- c is the speed of light in air (3×10^8 m/s)
- t is the ToF in seconds (laser to target and back to detector)

Range resolution is inversely proportional to the combined rise time of the laser, TIA and detector, while the maximum range is proportional to peak laser power and the combined sensitivity of the TIA and detector for the given optics. This indicates that to achieve high resolution over long distances, the system should have a high-peak-power laser with a fast rise time measured by a high bandwidth, low-noise photo diode, TIA, and detector. Additionally, the system must account for the return signal amplitude, which decreases proportionally to the square of the measured distance. The finite rise time of the measured return must also be accounted for in the detector to prevent level-dependent triggering errors.

TDC-based systems must solve the previously mentioned problems directly in the analog domain, which implies that fast rise time pulses and high receive bandwidth are required. The receive path also generally requires automatic gain control (AGC) to account for the return signal level and a time discriminator to ensure triggering occurs at a constant point in the rise of the return signal.

A high-speed ADC based system has a number of performance advantages over those based on a TDC. Because the ADC digitizes the return signal (instead of simply measuring time), signal processing can be employed to implement sophisticated detection schemes that not only have better performance than the TDC, but also provide additional information for target identification. This result allows for the relaxation of the laser rise time or improvement in range resolution for the same rise time. The wide dynamic range of the ADC eases and in some systems even eliminates the requirement for AGC in the receive path.

2.3.2 Phase-Shift Method Overview

An alternative to pulsed ToF is the phase shift ToF method, where the laser output power is AM modulated with a continuous wave (CW) signal. The phase difference between the transmitted and received signal is measured and distance is estimated using Equation 2. As with pulsed ToF measurements, the range resolution is directly proportional to the CW stimulus frequency if the phase error tolerance has been held constant. The repetitive nature of a CW signal creates the potential for aliasing if the distance exceeds the maximum unambiguous range described by Equation 3, which creates a tradeoff between range and resolution. This problem can be mitigated by using two different CW frequencies, one of lower frequency that provides range and the other of higher frequency that provides resolution.

$$d = \frac{c \times \Theta}{4 \times \pi \times f} \tag{2}$$

where

- d is the distance in meters
- c is the speed of light in air (3×10^8 m/s)
- θ is the phase angle in radians between the transmitted and received signals
- f is the frequency of the CW of the transmitted signal

$$r = \frac{c}{2 \times f} \tag{3}$$

where

- r is the maximum unambiguous distance in meters
- c is the speed of light in air (3×10^8 m/s)
- f is the frequency of the CW of the transmitted signal

The measuring phase can be accomplished a number of ways including the use of a heterodyne receiver and a high-speed ADC. With the heterodyne receiver method, a local oscillator (LO) is mixed with both the transmitted CW and the received return signal. The phase difference between these two intermediate frequencies (IFs) can be measured with low-speed ADCs. Direct sampling of the return signal with a high-speed ADC has a number of significant advantages over the heterodyne receiver. Firstly, the broadband nature of high-speed ADCs allows the simultaneous reception of multiple CW frequencies so that both range and resolution can be achieved at the same time. Removing the LO generator, mixers, and bandpass filters required with the heterodyne receiver not only reduces the cost and complexity of the system, but also eliminates the performance limitations that RF receivers experience, such as receiver linearity, transmitter and receiver crosstalk, and dynamic range. As with the pulsed ToF method, the high-speed ADC generally also eliminates much of the requirement for AGC and makes target detection more straightforward.

2.3.3 Overview of Pulsed ToF With Phase-Shift-Based Estimation Method

This design uses a pulsed ToF stimulus with a phase shift range estimation algorithm based on a high-speed ADC signal chain. Pulsed ToF has the advantage of producing high peak, but low average optical power, which is important for systems that must adhere to eye safety requirements. A pulsed laser driver is also generally more straightforward to implement, which results in reduced system complexity and cost. The discrete Fourier transform (DFT) is used to estimate the phase of both the reference and return signals, the delta of which can be used to calculate distance as with the phase shift method (using Equation 2).

Figure 3 shows the stimulus used, where N narrow pulses are transmitted in each frame and the return and reference signal are both coherently digitized with a capture synchronized to the transmitter. A subset of the digitized samples equivalent to exactly N periods are selected for processing (see Figure 4). The sample window is chosen in such a way to include all N periods of the reference and return signal. This implies a maximum ambiguous range as noted with the phase shift method that must be accounted for, which can be controlled by setting the period of the pulses.

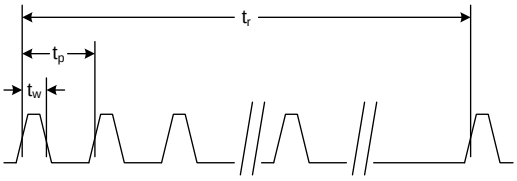

Figure 3. Laser Stimulus Waveform

The pulse width, t_w, is selected to be just wide enough that the pulse can be sampled with a few samples. The pulse period, t_p should be selected such that both the maximum unambiguous distance requirement is met and the filtered TIA output has time to settle. The number of pulses per frame impacts the standard deviation of the measurement. Increasing the number of pulses reduces the standard deviation and the expense of higher average power. The variable t_r sets both the frame rate and average power of the laser.

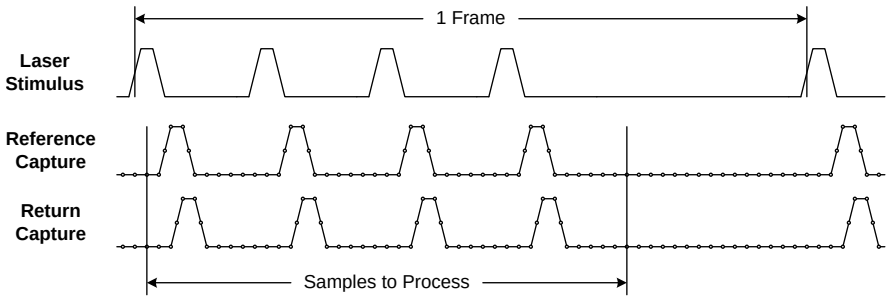

Figure 4. Captured Reference and Return Waveforms

The return and reference sample set are processed using a non-windowed DFT. The phase of the fundamental or one of the harmonics of the reference is then subtracted from that of the return. This is then converted to distance using Equation 2 and scaled for gain and offset based on calibration data (see Figure 5).

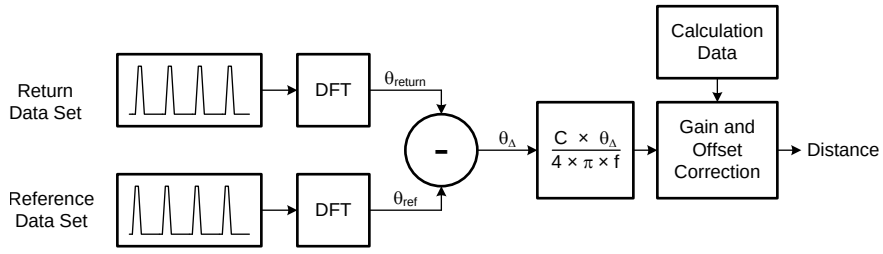

Figure 5. Distance Calculation Algorithm

For this design, pulse width, t_w, has been set to 30 ns, which results in about seven ADC samples per pulse after filtering. A period, t_p has been set to 512 ns to ensure that the filtered TIA output settles between pulses and ten pulses transmitted per frame. The frame has been set to 2 ms so that the average laser power is less than 1 mW. For each measured frame, 640 samples are taken for the capture after the trigger. After taking the DFT, the phase in Fourier bin 20 (which corresponds to the second harmonic of the pulse train) is taken for both reference and return and then processed with gain and offset correction to produce a distance measurement. The second harmonic was selected because it showed the lowest mean range error and standard deviation for this design.

2.3.4 System Construction

2.3.4.1 Optical Driver and Receiver Board

Figure 6 shows a block diagram of the optical driver and receiver board, which comprises a laser driver, laser diode, collimation and focusing optics, and reference-and-return photodiode receive circuits. The board is powered by a 6-V supply for the photodiode receiver circuit and a 10-V supply for the laser driver circuit, which each have 3.3-V voltage regulators for low-voltage portions of the circuits. SMP coaxial connectors are used to connect the inputs and outputs to the other boards in the system.

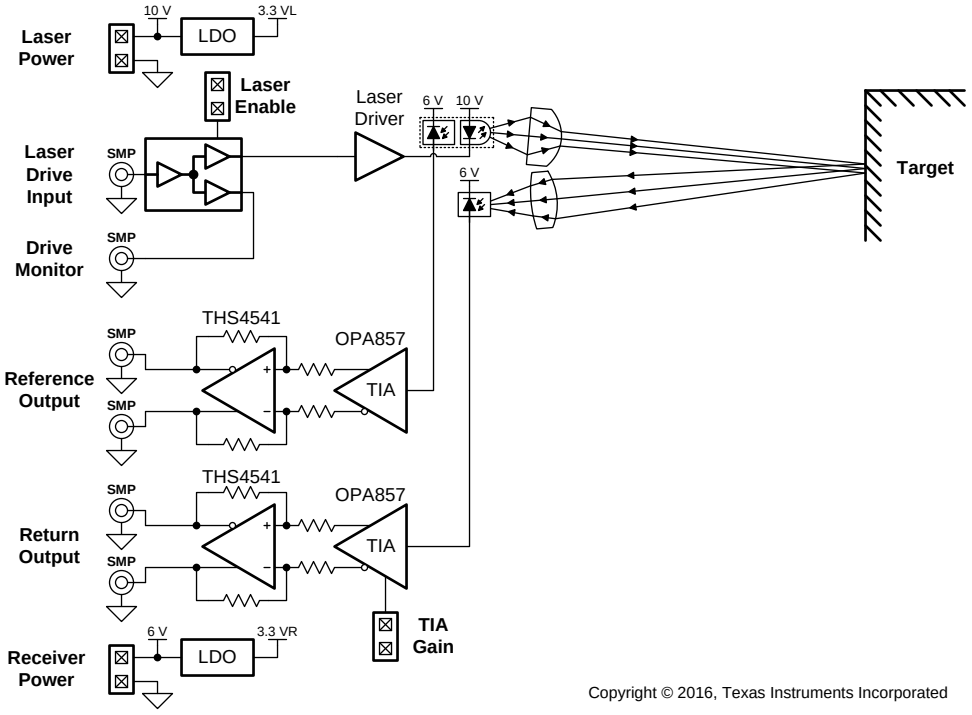

Figure 6. Optical Driver and Receiver Board Block Diagram

Figure 7 shows the front side of the optical driver and receiver board, which houses the laser diode and reference and return photodiodes. Collimation and focusing optics are attached to the board through lens tube mounting flanges.

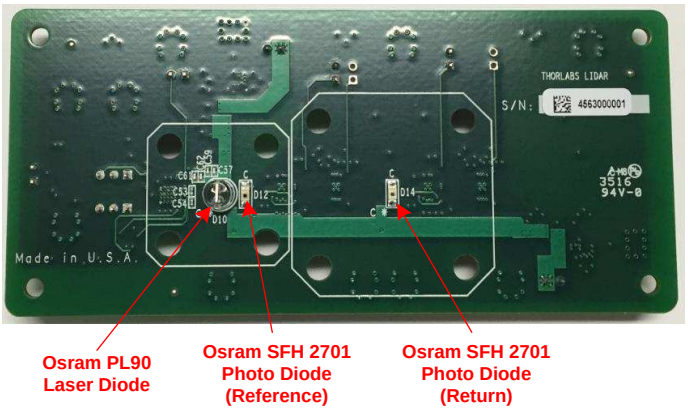

Figure 7. Optical Driver and Receiver PCB—Front View

Figure 8 shows the back side of the board, which houses all of the active circuitry. The *TIA Gain* for the return channel and *Laser Enable* are controlled through jumpers.

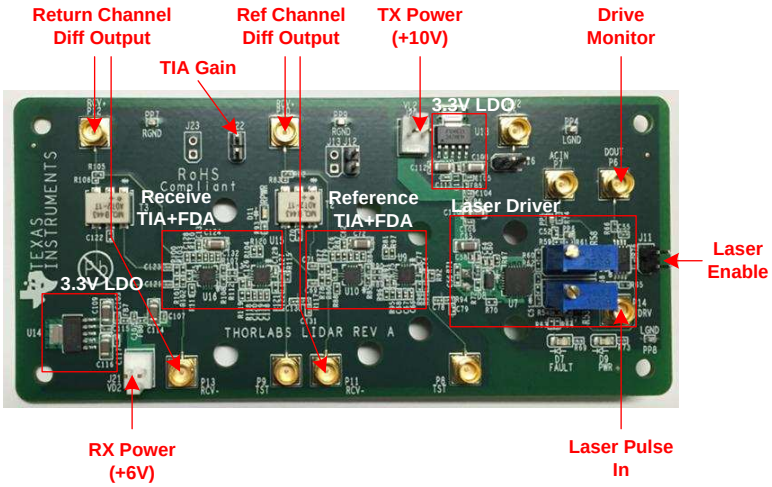

Figure 8. Optical Driver and Receiver PCB—Back View

2.3.4.2 DAC Source and ADC Capture Board Setup

Figure 9 shows the setup TSW3070 (DAC5682Z), ADC3244 EVM and two TSW1400 controller boards. Each board has a USB and DC wall-adapter power connection. Additionally, the SYNC output of the DAC TSW1400 is connected to the TRIGGER input of the ADC TSW1400 through an SMA coax cable, which synchronizes the source and capture. The 125-MHz CLK output of the TSW3070 drives the clock input of the ADC3244 EVM through an SMA coax cable. The TSW3070 receives a 15-dBm, 1-GHz clock input from a RF signal generator through an SMA coax cable.

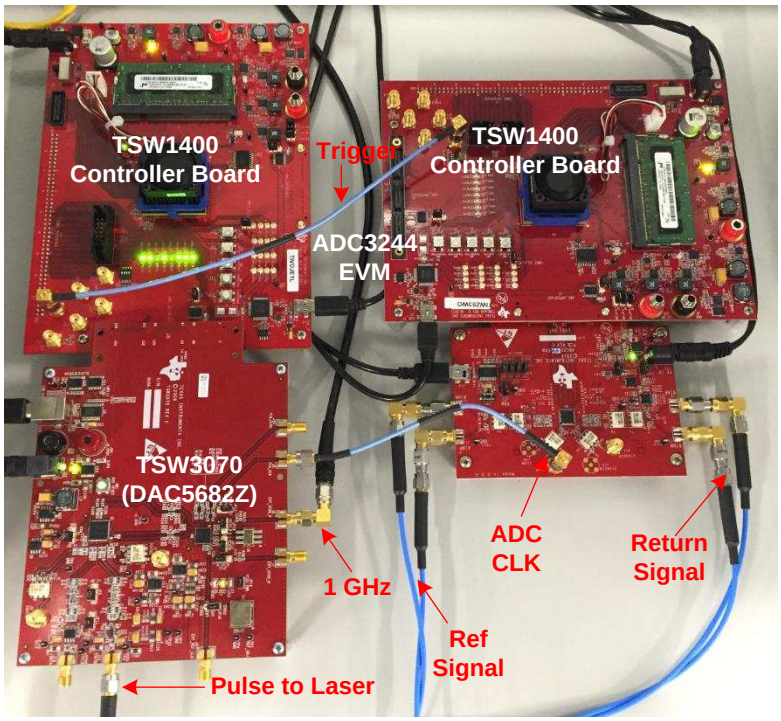

Figure 9. DAC Source and ADC Capture Board Setup

The DAC output of the TSW3070 and reference and return differential inputs to the ADC3244 connect to the optical driver and receiver board through SMA-to-SMP coax cables.

2.3.5 Optics

This design uses off-the-shelf optics and mounting components from Thorlabs to demonstrate collimation of the laser and focusing of the return signal onto the photodiode. Figure 10 shows a cross section of the optics along with the laser diode and photodiodes. These components have been selected to balance a number of design objectives while retaining a straightforward implementation. The laser driver and reference and return receivers have been implemented on a single printed-circuit board (PCB) with optics attached through flanges.

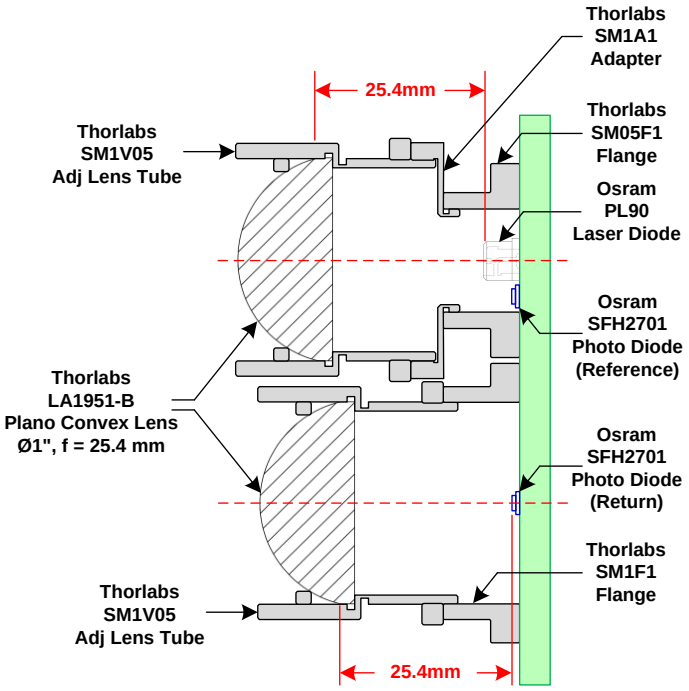

Figure 10. Cross Section of Optics

A 0.5-in flange (SM05F1) is used along with a 0.5-in to 1.0-in adapter (SM1A1) for the laser optics so that the laser and receiver lens tubes can be mounted as close together as possible. This is important because it determines the minimum range where the field of view (FOV) of the receiver includes the laser beam. Both driver and receiver optics use adjustable lens tubes with locking rings (SM1V05), which makes collimation of the laser and focusing of the return straightforward. The holes in the PCB for the flanges are drilled oversized to facilitate alignment.

2.3.5.1 Collimating Lens

Laser diodes typically produce highly divergent light, which is not very useful for distance measurement applications. The process of collimation takes the fan of light rays from the laser diode emitter and straightens them out into a narrow beam. Because the laser has an emitter with a finite aperture size (that is, it is not a perfect point source), some residual divergence remains after collimation. Figure 11 shows the collimation process and Equation 4 and Equation 5 show the trade-off between beam width and divergence for a given emitter aperture size.

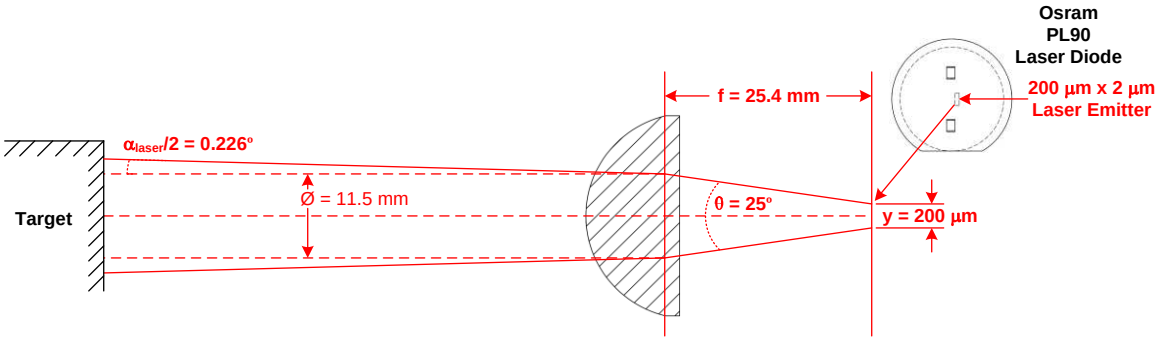

Figure 11. Collimation of Beam

$$\varnothing_{laser} = 2 \times f \times TAN\left(\frac{\theta}{2}\right) + y \quad (4)$$

where

- $\varnothing_{laser}$ is the beam width in mm
- f is the focal length in mm
- θ is the beam laser divergence angle in °
- y is the laser emitter aperture length in mm

$$\alpha_{laser} = 2 \times ATAN\left(\frac{y}{2 \times f}\right) \quad (5)$$

where

- α_{laser} is the beam divergence angle in °
- y is the laser emitter aperture length in mm
- f is the focal length in mm

The OSRAM PL90 laser diode has been selected for its ability to generate high-peak-power pulses with a fast rise time. This laser diode has an aperture of 200 µm × 2 µm with a divergence angle of 8° parallel to the emitter and 25° perpendicular to the emitter. For beam width and divergence calculations, the longer of the two aperture dimensions (200 µm) and the larger of the two divergence angles (25°) are used for y and θ respectively.

A Thorlabs LA1951-B 1-in diameter Plano-Convex lens with a 25.4-mm focal length has been selected to collimate the laser. This focal length balances beam width and divergence angle given the relatively large emitter width of 200 µm and the desire to keep the distance between the laser and receiving photodiode as small as possible. The Plano-Convex lens profile is commonly used for collimation and has been selected over more expensive spherical and best form profiles because they did not offer any significant advantages. The lens has an anti-reflective coating appropriate for 905-nm operation which improves the optical output of the collimated beam.

Using this setup, a beam width of 11.5 mm with a divergence angle of 0.226° has been achieved. At 9 m, this yields a beam width of about 82.5 mm, which is still quite usable for ranging. Increasing focal length lessens the spreading of the beam because of divergence, but increases the beam diameter. The usable aperture of the Plano-Convex lens is about 90% of its diameter, which implies that the focal length could be increased to approximately 50 mm with a beam width of 22.4 mm.

Figure 12 shows a cross section of the collimating optics setup. The alignment process involves adjusting both the placement of the SM05F1 mounting flange and lens focus through the SM1V05 adjustable lens tube. Because the output of the laser diode is invisible near infrared light, a Thorlabs VRC4 detector card is used to make the beam visible during the alignment process. This card has a photosensitive coating which emits green light when illuminated by the laser.

Because the laser aperture has a wide aspect ratio (200 µm × 2 µm), the collimated beam results in a thin rectangle instead of a round spot. The lens focus is adjusted until a small rectangle is visible on the detector card that diverges minimally as the range increases. When the beam is roughly collimated, the flange position is adjusted such that the beam is focused on the center of the target.

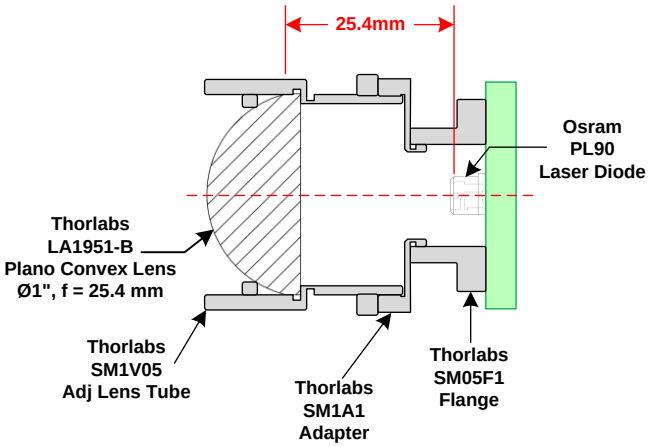

Figure 12. Collimating Optics Cross Section

2.3.5.2 Focusing Lens

Light returning from the target is focused by a Thorlabs LA1951-B 1-in diameter Plano-Convex lens onto a OSRAM SFH2701 PIN photodiode using an assembly that Figure 13 shows. The diameter of the focusing lens determines its light-collecting ability, while focal length sets the FOV. Placing the laser close to the receiver is desirable so that its FOV includes that of the laser at close range; however, there is a trade-off between light-collecting ability and close range capability. To further improve the light-collecting capability, a lens with an anti-reflective coating active in the NIR region has been selected.

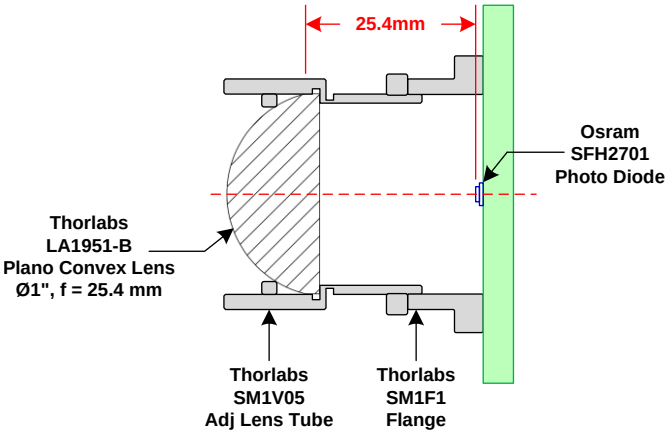

Figure 13. Focusing Optics Cross Section

The OSRAM photodiode used for this design has an active detecting region of 600 µm × 600 µm. To maximize the received signal, the lens is aligned and focused to a spot size that just covers all of the active region of the detector, which yields a diameter of approximately $\sqrt{2}$ × 600 µm = 850 µm. When combined with the focal length of the lens, a FOV can be determined by using Figure 14. The FOV angle is chosen to be larger than the divergence angle of the laser (0.452°) so that all of the return light can be collected. With a 25.4-mm focal length and spot size of 850 µm, a FOV angle of 1.92° is achieved. This angle is significantly larger than that of the laser, which eases focusing and alignment while delivering the ability to operate at ranges less than 2 m.

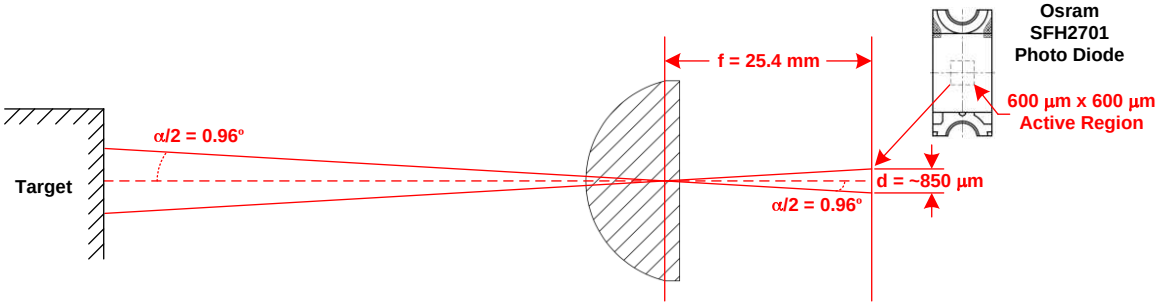

Figure 14. Receiver Field of View

$$\alpha = 2 \times \text{ATAN}\left(\frac{d}{2 \times f}\right) \quad (6)$$

where

- α is the FOV in °
- d is the diameter of a circle incorporating the active region of the photodiode in mm
- f is the focal length in mm

A number of lens profiles are appropriate for focusing, including Plano-Convex, best form and spherical. The Plano-Convex is the most economical lens profile and the improved spherical aberration performance of best form profile and shorter possible focal length of spherical profiles did not offer improvements for this application. If outdoor operation is desired, an optical filter can be added to the receive lens tube to reduce the impact of sunlight.

2.3.6 Laser Transmit Path

2.3.6.1 High-Speed Transmit Signal Chain

The DAC5682Z is operated at 500 MSPS with no interpolation. A 1-GHz signal generator drives the CDCM7005 clock synchronizer and PLL, which is used as a clock divider to produce all the clocks for the system. As Figure 15shows, the DAC receives 500 MHz (divide-by-2), the ADC receives 125 MHz (divide-by-8), and the TSW1400 receives 250 MHz (divide-by-4). The clock for the ADC EVM is taken from the TSW3080 clock output.

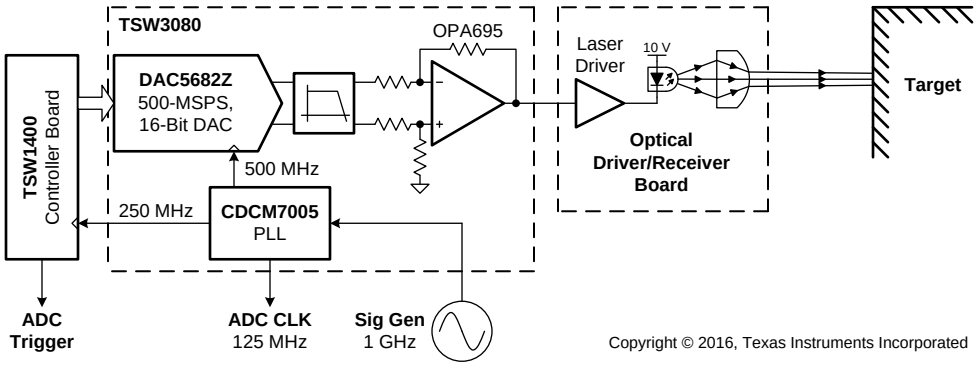

Figure 15. HS Transmit Signal Chain

The TSW1400 controller board is used to provide stimulus to the DAC through a waveform stored in its memory. This waveform is looped continuously with a trigger being generated at the beginning of each cycle, which is sent to the second TSW1400 used for capturing the ADC results. The output of the DAC is low-pass filtered before being converted into a voltage by the OPA695 high-speed op amp. This signal is driven through a coax cable to the optical driver and receiver board, where it is connected to the laser driver input. The laser driver applies current pulses into the laser, which is then collimated and aligned with the target.

2.3.6.2 High-Speed DAC Antialiasing and I-V Conversion

The DAC5682Z produces a differential current output that must be filtered and converted into a single-ended voltage before driving the laser. The circuit that Figure 16 shows is composed of a passive termination and a 200-MHz low-pass filtering network that drives an OPA695 based, high-speed difference amplifier. To produce a 3-V_{pk} output, the gain of the difference amplifier was increased by changing R86 and R94 from 499 Ω to 1499 Ω.

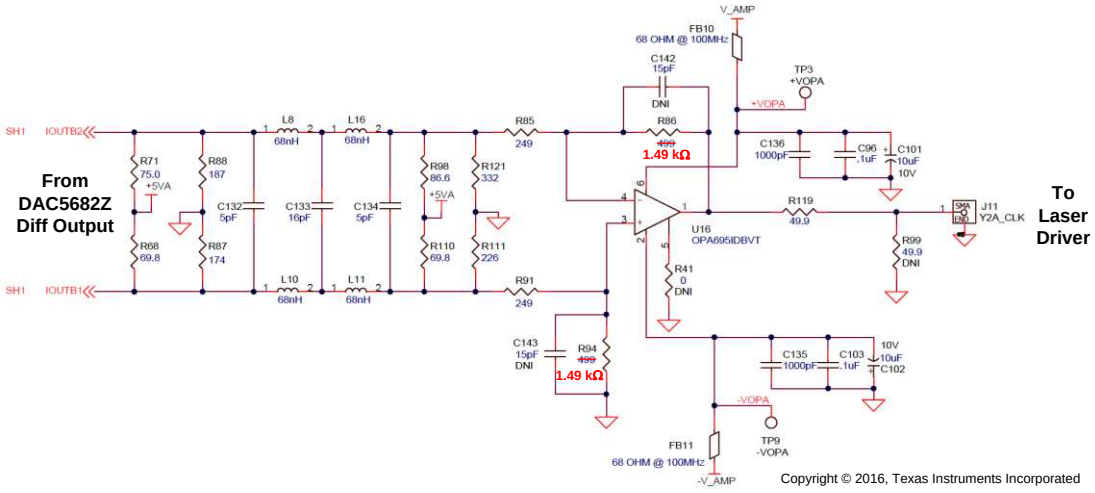

Figure 16. DAC Driver Circuit

For more information on this circuit, refer to TSW3070 High Speed DAC Demonstration EVM.

2.3.6.3 Laser Driver

The iC-HG laser driver IC from iC-Haus has six switchable, high-speed current sources capable of delivering up to 1.5 A_{pk} each (or 500-mA DC). The sink current level on the LDKx is proportional to the voltage on the CIx when ENx is asserted high (and zero when ENx is low). As Figure 17 shows, the first five channels are connected in parallel and the sixth is reserved for optional DC biasing. Output current is set by adjusting the *Laser Drive Level* and *Bias Level* multi-turn potentiometers. A CDCLV1102 clock fan-out buffer is used to drive EN1-EN5 with a copy sent to the *Drive Monitor* output, which is useful for triggering an oscilloscope during alignment and focusing. A jumper is provided to control the enable of the driver through the clock fan-out buffer.

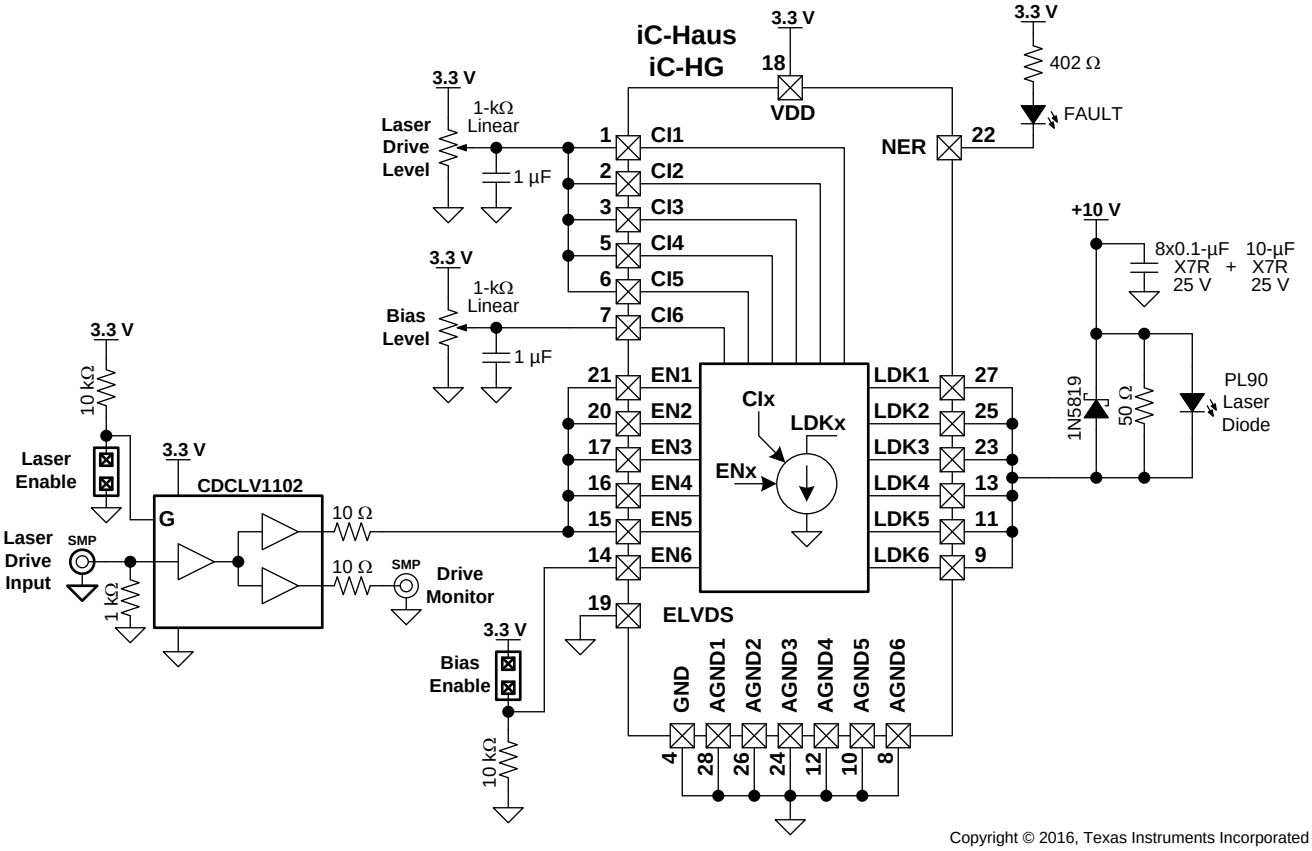

Figure 17. Laser Driver Circuit

The 10-V laser diode supply is bypassed by eight parallel 0.1-uF bypass capacitors close to the laser diode to provide the high dynamic current required to generate a short pulse. A Schottky diode and 50-Ω resistor are placed in parallel with the laser diode to prevent voltage spikes due to reverse recovery when the current has been turned off. The layout has been carefully arranged to minimize the loop area formed by the supply (including bypassing) laser diode, output, and ground.

This design does not require biasing of the laser diode, so the *Bias Enable* jumper has been removed, which disables the sixth current source. The *Laser Drive Level* is adjusted to produce 6-A current pulses, which equates to about 5.75 W of laser output power. The pulse parameters are set to keep the laser average power less than 1 mW.

2.3.7 Photodiode Receive Path

2.3.7.1 High-Speed Receive Signal Chain

Figure 18 shows a block diagram of the high-speed receive signal chain, which measures both the light emitted by the laser and that returning from the target. This measurement allows the system to calculate the delta in the time between when the laser fired and when the signal returned. For the reference channel, a small amount of the light emitted by the laser illuminates its photodiode, which produces a weak current that is amplified by the OPA857 high-speed TIA. This amplified signal is then further amplified by the THS4541 high-speed FDA before traveling through a pair of coax cables to the ADC3244 EVM. On the EVM, the differential signal drives a second unity gain THS4541 FDA before being filtered and captured by the ADC3244.

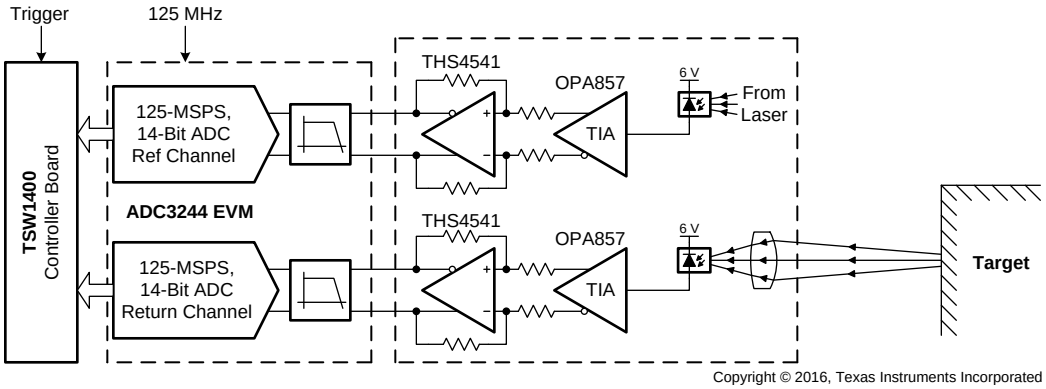

Figure 18. High-Speed Receive Signal Chain

The return channel operates the same as the reference, except a lens is used to focus light returning from the target. Note that if the receive circuitry is located on the same circuit board as the ADC, only one FDA per channel is required.

2.3.7.2 Reference and Return Path TIAs

Figure 19 and Figure 20 respectively show block diagrams of the return and reference path TIA and FDA. The OSRAM SFH 2701 photodiode is reverse-biased by a 6-V supply with its anode connected to the input of the OPA857 TIA. When light strikes the active region of the photodiode, a small current is generated, which is converted to a voltage by the OPA857 device. Installing the gain selection jumper lowers the gain by paralleling the 5-kΩ and 20-kΩ feedback resistors. The output of the TIA and its mid-rail reference are connected to a THS4541 device configured for a differential gain of 5 and an output common mode set to half of the 3.3-V supply. The differential output of the THS4541 device drives SMP coax connectors through a 50-Ω source termination.

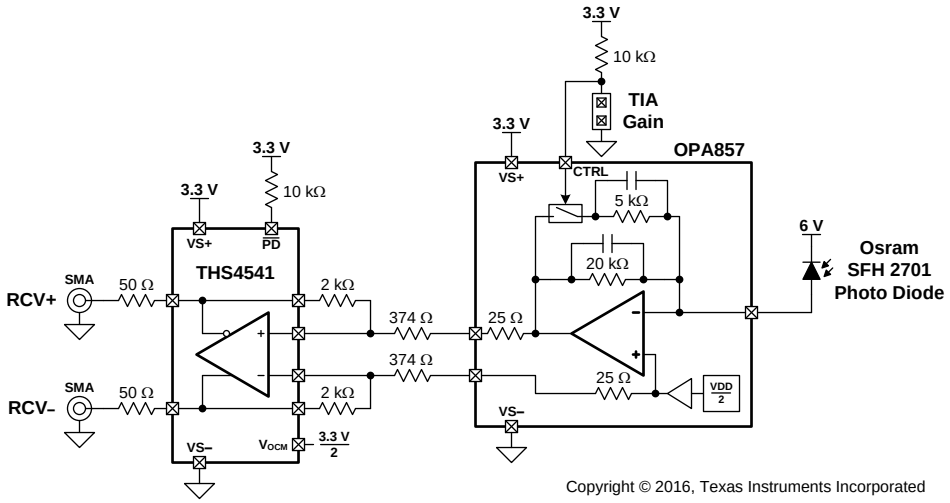

Figure 19. Return Path TIA

The reference path photodiode experiences a higher optical level than the return path, so the TIA gain is reduced by adding external resistors between the output and input. The TIA gain control is grounded to put the internal 5 kΩ in parallel with the 20-kΩ resistors. This implementation gives an approximate feedback resistance of 1.33 kΩ. The feedback resistance is split in half to reduce the parasitic capacitance experienced by both the output and input. The 0.1-pF capacitors are added to reduce the peaking at high frequencies.

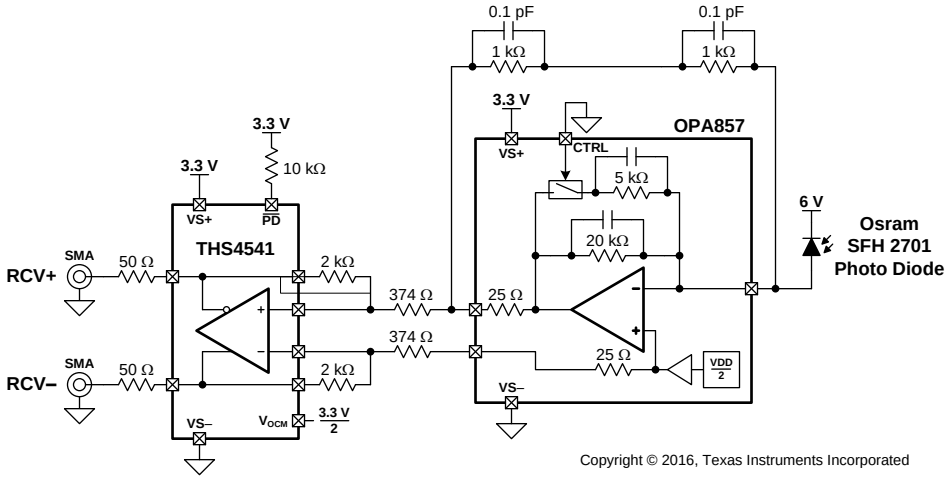

Figure 20. Reference Path TIA

For more information on this circuit, refer to the Reference Design for Extending OPA857 Transimpedance Bandwidth [2].

2.3.7.3 ADC Antialiasing and Driver Amplifier

The ADC3244 EVM has options for a transformer-coupled path and DC-coupled path. For this design, the DC-coupled path has been selected (see Figure 21), which contains a THDS4541 FDA and 40-MHz Bessel low-pass filter. To select the DC-coupled path, remove R3, R4, R14, R18, R139, and R142 then populate R120, R121, R135 through R138, R141, and R144 with 0-Ω resistors (see Figure 21).

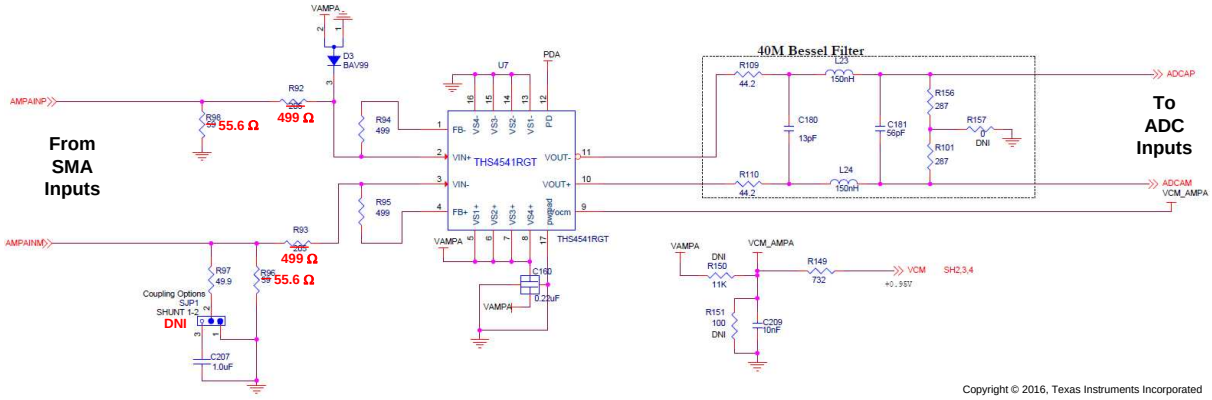

Figure 21. ADC Antialiasing and Driver Amplifier

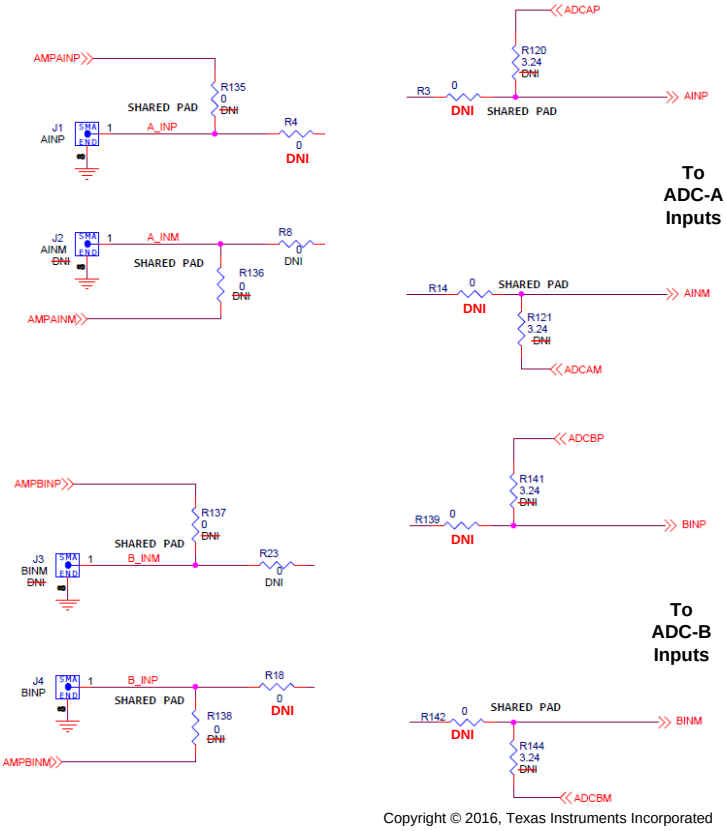

Figure 22. Selecting DC-Coupled Path on ADC3244 EVM

A differential input has been used, so the SJP1 and SJP2 soldered jumpers are removed and end launch SMAs J2 and J3 are installed. The THS4541s differential gain has also been reduced from 2 to 1 by changing R92, R93, R127, and R128 from 205 Ω to 499 Ω and R98, R96, R133, and R131 from 59.0 Ω to 55.6 Ω. For more information on this board, refer to the ADC3244 Evaluation Module.

3 Testing and Results

3.1 Setup

Range measurements were taken in a laboratory setup with the optical driver and receiver board held stationary using a Thorlabs optical breadboard and pedestal mount as Figure 23 shows . Several sheets of white printer paper attached to a stand were used as the target, which is both highly reflective and diffusive. The target was held perpendicular to the lab bench at a constant distance from the edge of the bench such that the range could be adjusted using a tape measure affixed to the bench. Adjustment of the optical breadboard was made such that the beam fired along the axis of the tape measure parallel to the lab bench (that is, at a constant heigh from the lab bench surface). An oscilloscope was used during the alignment and focusing process.

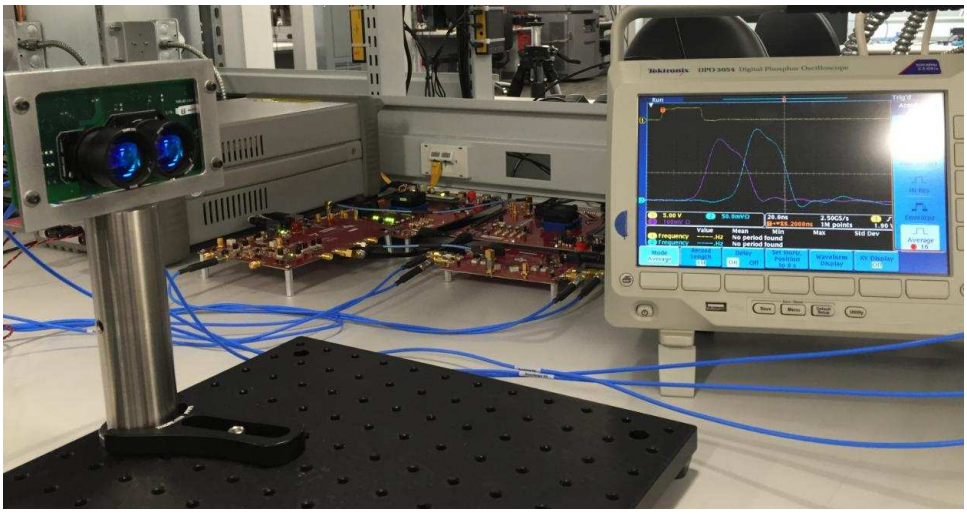

Figure 23. Laser Range Measurement Setup

3.2 Loading and Running DAC Waveform

The DAC5682Z GUI is used to configure the settings such that the DAC can operate with its PLL bypassed and with no interpolation. The GUI is also used to configure the CDCM7005 as a clock divider for the various clocks in the system. Figure 24 shows the settings required to achieve this with the DAC.

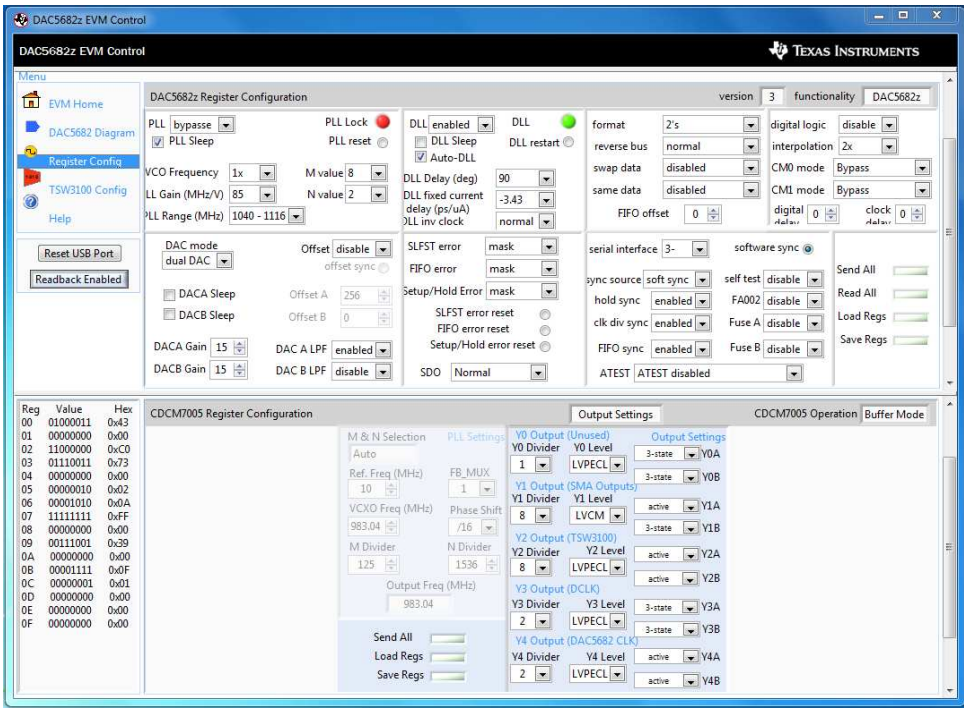

Figure 24. DAC5682Z GUI

When the DAC has been configured, HSDC Pro is used to load and run the laser stimulus waveform. Figure 25 shows the loaded waveform in HSDC Pro. The DAC5682Z setting is selected and then *Data Rate* is set to 500 MSPS with a 2's complement data format. Finally, the stimulus file is loaded using the *Load External File* button. Clicking the *Send* button loads the waveform and starts the playback of the waveform.

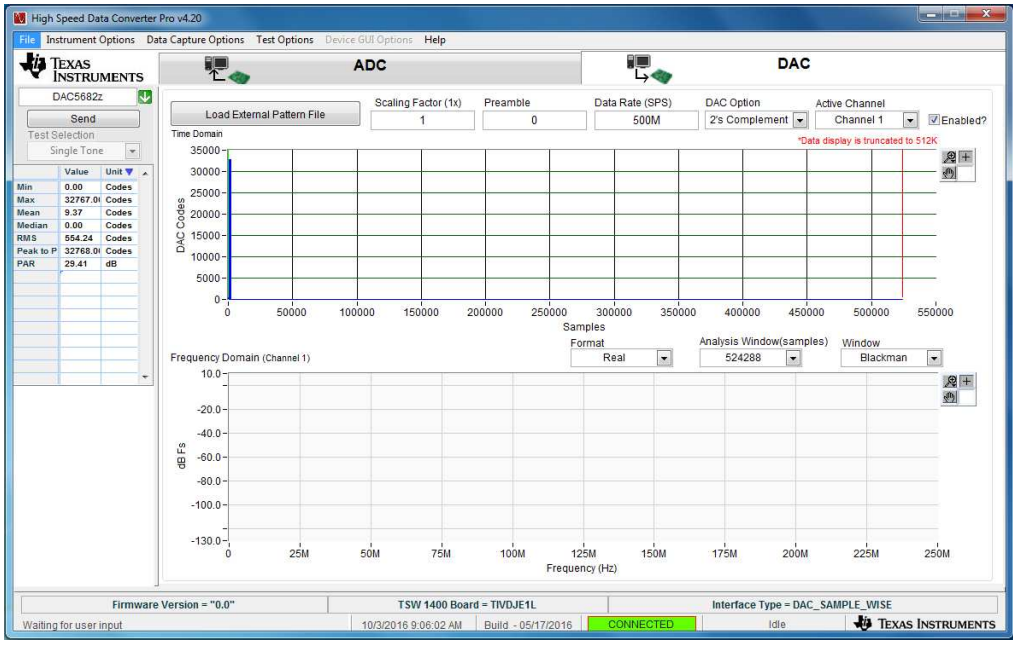

Figure 25. Loading DAC Waveform With HSDC Pro

3.3 Optical Alignment, Collimation and Focusing

When the DAC has been configured to generate the stimulus waveform, the laser must first be collimated and then aligned. Collimation is accomplished by adjusting the distance between the laser diode emitter and the collimating lens using the threads on the adjustable lens tube. As Figure 26 shows, a Thorlabs VRC4 detector card was used to make the 905-nm light from the laser visible. The lens tube was adjusted until the spot produced had a bright rectangular shape that had a minimal increase in size as the card was moved away from the emitter.

Figure 26. Oscilloscope Capture of Reference and Return Signal

To align the laser, the flange-mounting screws were loosened such that the flange position is adjustable. The detector card was placed at a range of approximately 2 m and the flange position was adjusted until the center of the beam was located in a position on axis with the emitter. Alignment was further refined as range was increased such that movement of the center of the laser spot on the card was minimized. The mounting screws were then tightened to lock the alignment of the laser.

Alignment and focusing of the receiver lens was accomplished in a similar fashion as collimation. An oscilloscope, triggered by the pulse monitor output of the driver and receiver board, was used to monitor the output of the received return pulse during adjustment, as Figure 27 shows. An iterative process of adjusting alignment and focus was repeated until the strongest return signal could be obtained at 5 m.

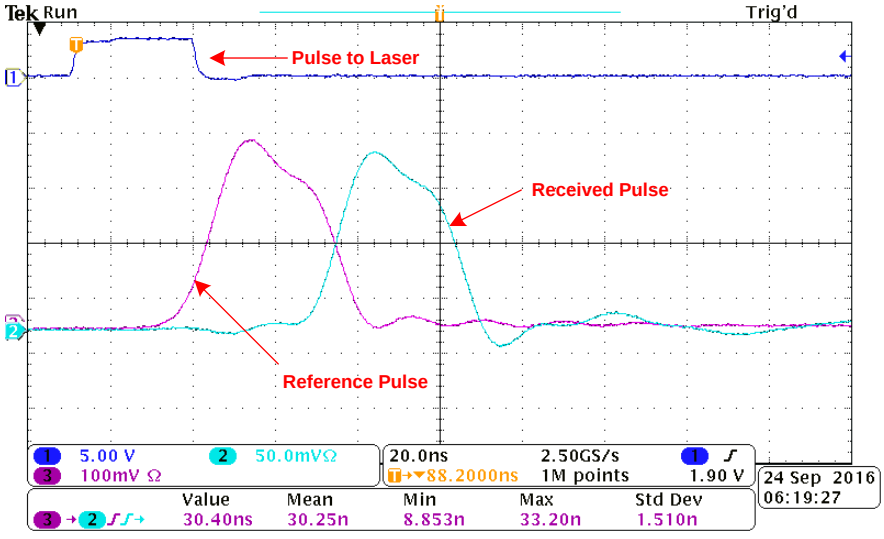

Figure 27. Oscilloscope Capture of Reference and Return Signal

3.4 Configuring ADC and Capturing ADC Results

After powering up the ADC3244 EVM, the reset button on the board must be pressed to reset the ADC. The GUI can then be launched where the dither and chopper functions are disabled by checking the four boxes as Figure 28 shows.

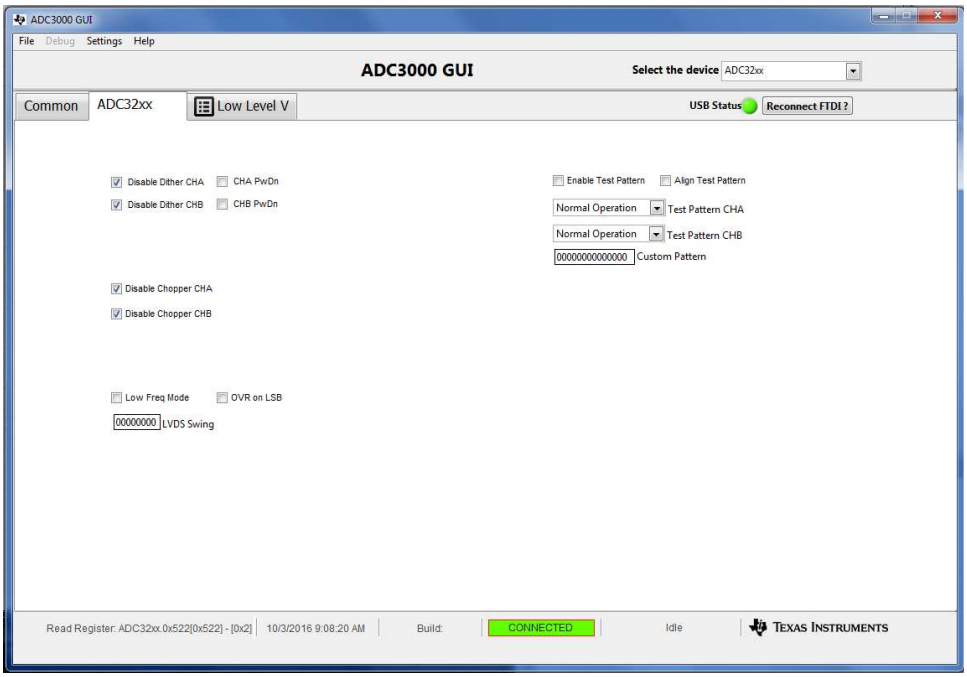

Figure 28. ADC3244 GUI

Next, the HSDC Pro software is launched, which connects to the TSW1400 controller board. The *ADC324x_2W_14bit* device is selected with the *ADC Output Rate* set to 125 MHz. Triggering is enabled by clicking the *Trigger mode enable* check box in the *Trigger Option* menu under *Data Capture Options* (see Figure 29). Because of the low refresh rate, only one frame is captured during each acquisition.

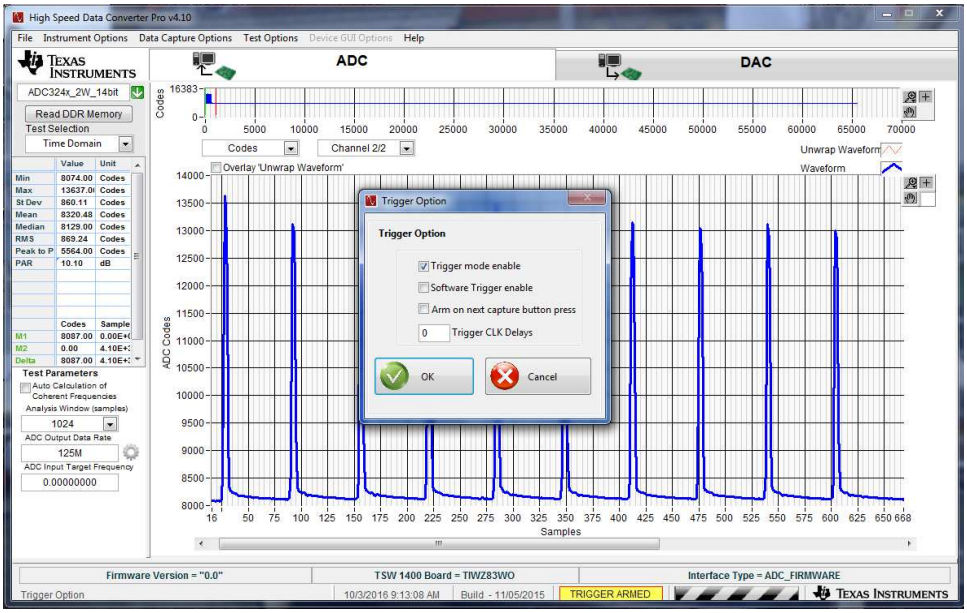

Figure 29. Trigger Setup

Figure 30 and Figure 31 show the capture of the reference and return signal, respectively.

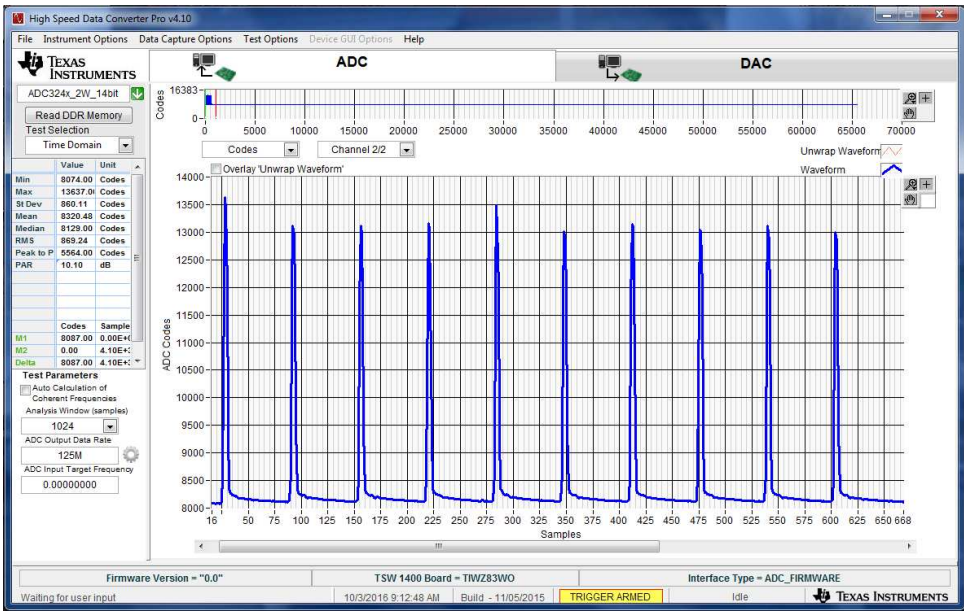

Figure 30. Captured Reference Signal

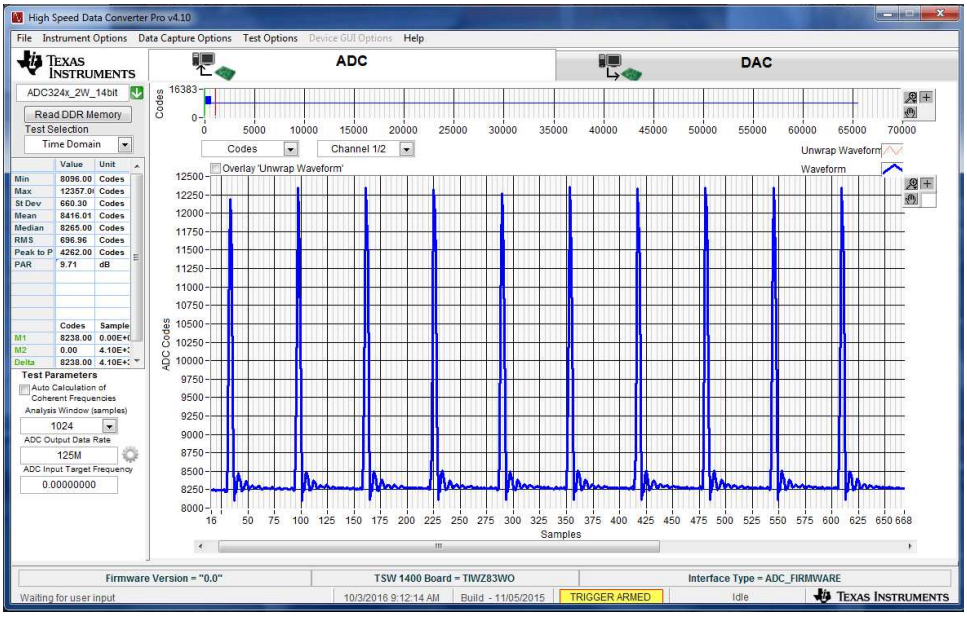

Figure 31. Captured Return Signal

Each capture was saved and processed to calculate range.

3.5 Range Results

Distance was measured from 1.5 m to 9 m using a white printer paper target with the laser adjusted to produce ≈5.75-W pulses. Each frame was composed of ten 30-ns pulses spaced 512 ns apart. A 2-ms frame rate was selected to keep the average power under 1 mW. 128 frames were collected at each distance where range mean and standard deviation were calculated after correcting for gain and offset. Figure 32 shows the resulting measured range versus range.

The lower TIA gain setting was used from 1.5 m to 3 m and the higher setting was used from 3 m to 9 m. During initial data collection, it was determined that the ADC EVMs 40-MHz Bessel filter did not have sufficient attenuation at the Nyquist and beyond, which caused degradation in the range mean and standard deviation performance due to aliasing. Mini-Circuits LPF-BP50+ filters were installed on each ADC input, which eliminated this issue. A steeper filter response, such as a Chebychev, is also sufficient in this application for solving this problem.

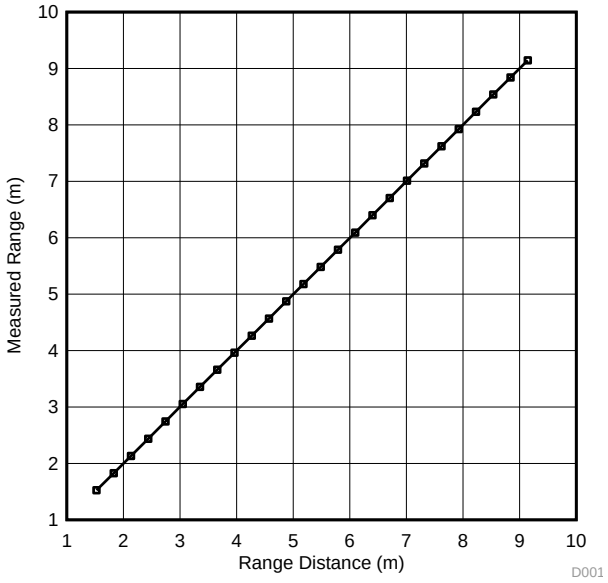

Figure 32. Measured Range versus Range

Figure 33 shows the standard deviation of the measured mean of the range versus range. The dip at 3 m was the result of the increase of the TIAs gain, which reduced the input-referred noise floor. The increase of standard deviation with range can be directly attributed to the reduction in the signal-to-noise ratio (SNR), which is the result of the received amplitude decreasing proportionally to the square of range.

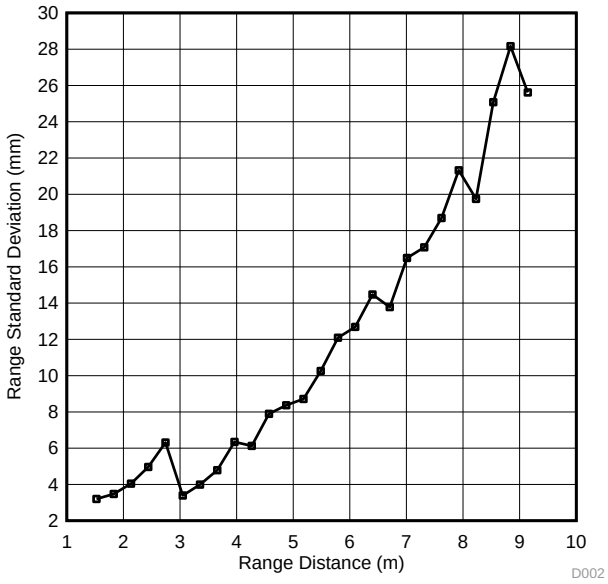

Figure 33. Range Standard Deviation versus Range

Figure 34 shows the range error in the mean versus range. This error can be attributed to a number of factors including the precision of the measurement setup, crosstalk between the driver and receiver, and residual aliasing in the ADC path. The maximum range error of 5.5 mm corresponds to a time error of ±37 ps, which demonstrates that even with a 125-MSPS ADC, time estimates substantially less than the sample period can be estimated.

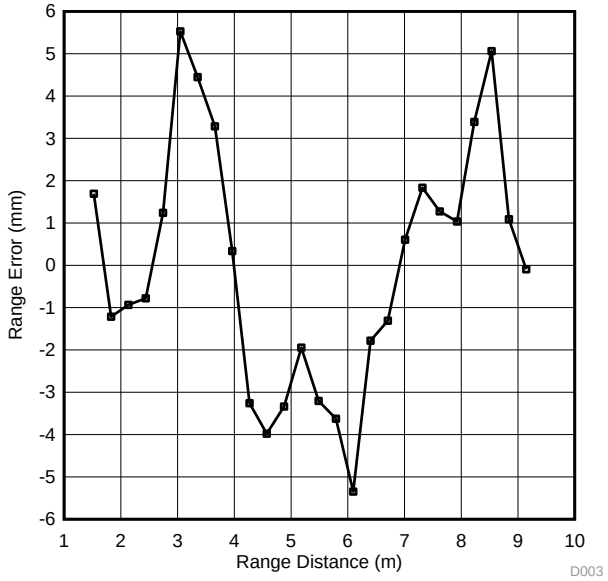

Figure 34. Range Error versus Range

Figure 35 compares the attenuation versus range for white printer paper, brown cardboard, black powder coated steel and Thorlabs black optical masking tape. Attenuation is shown relative to the level received with the white printer paper at 2.13 m. This relation shows that the received signal attenuation is proportional to the square of distance for diffusive materials regardless of the reflection coefficient. This amplitude information provides information useful in target detection because the amplitude at a given range is known for each type of material.

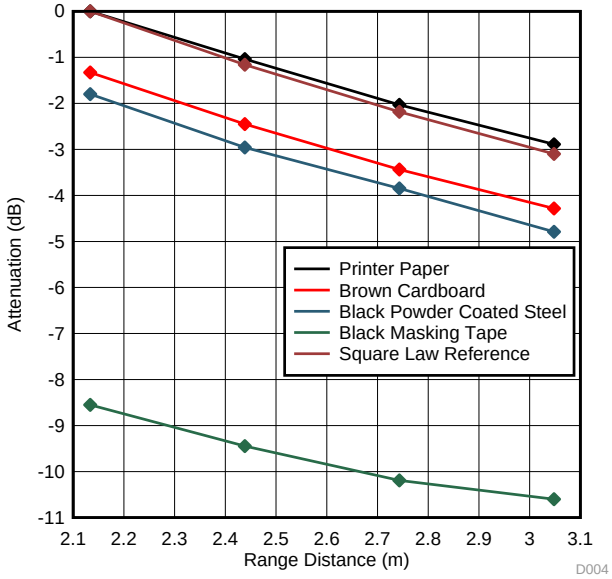

Figure 35. Attenuation versus Range

4 Design Files

4.1 Schematics

To download the schematics, see the design files at TIDA-001187.

4.2 Bill of Materials

To download the bill of materials (BOM), see the design files at TIDA-001187.

4.3 PCB Layout Recommendations

4.3.1 Layout Prints

To download the layer plots, see the design files at TIDA-001187.

4.4 Cadence Project

To download the Cadence project files, see the design files at TIDA-001187.

4.5 Gerber Files

To download the Gerber files, see the design files at TIDA-001187.

4.6 Assembly Drawings

To download the assembly drawings, see the design files at TIDA-001187.

5 Software Files

To download the software files, see the design files at TIDA-001187.

6 Related Documentation

1. Texas Instruments, *TSW3070EVM: Amplifier Interface to Current Sink DAC - Arbitrary Waveform Generator Demonstration*, User's Guide (SLWU055A)
2. Texas Instruments, *Reference Design for Extending Transimpedance Bandwidth of OPA857*, User's Guide (TIDUC73)

6.1 Trademarks

7 About the Author

DAVE GUIDRY is a member of the applications team in the high speed catalog converters group at Texas Instruments. He received his BSEE form Texas A&M University, College Station in 2001. Since graduation he has worked for Texas Instrument with roles in SOC characterization, production test development, test strategy, instrumentation design, analog IC design, systems and applications. Mr. Guidry is a Senior Member of TI's technical staff.

Revision History B

NOTE: Page numbers for previous revisions may differ from page numbers in the current version.

Changes from A Revision (February 2017) to B Revision	Page
• Changed measurement range specification from "1.5 m to 9 m" to "up to 9 m or greater"	1
• Added "Automotive Grade Versions Available for Select Devices" to *Features*	1
• Added Automotive Scanning LIDAR and Drones to *Applications*	1
• Reorganized order of sections; no changes to content	2
• Added content to *System Description* section: "The optics used in this design are optimized for up to 9 m of distance. A longer range is possible through a choice of optics."	3

Revision History A

Changes from Original (November 2016) to A Revision	Page
• Changed title from "*Optical Distance Measurement Reference Design Using Pulse Time of Flight*" to "*LIDAR-Pulsed Time-of-Flight Reference Design Using High-Speed Data Converters*"	1

IMPORTANT NOTICE FOR TI DESIGN INFORMATION AND RESOURCES

Texas Instruments Incorporated ('TI") technical, application or other design advice, services or information, including, but not limited to, reference designs and materials relating to evaluation modules, (collectively, "TI Resources") are intended to assist designers who are developing applications that incorporate TI products; by downloading, accessing or using any particular TI Resource in any way, you (individually or, if you are acting on behalf of a company, your company) agree to use it solely for this purpose and subject to the terms of this Notice.

TI's provision of TI Resources does not expand or otherwise alter TI's applicable published warranties or warranty disclaimers for TI products, and no additional obligations or liabilities arise from TI providing such TI Resources. TI reserves the right to make corrections, enhancements, improvements and other changes to its TI Resources.

You understand and agree that you remain responsible for using your independent analysis, evaluation and judgment in designing your applications and that you have full and exclusive responsibility to assure the safety of your applications and compliance of your applications (and of all TI products used in or for your applications) with all applicable regulations, laws and other applicable requirements. You represent that, with respect to your applications, you have all the necessary expertise to create and implement safeguards that (1) anticipate dangerous consequences of failures, (2) monitor failures and their consequences, and (3) lessen the likelihood of failures that might cause harm and take appropriate actions. You agree that prior to using or distributing any applications that include TI products, you will thoroughly test such applications and the functionality of such TI products as used in such applications. TI has not conducted any testing other than that specifically described in the published documentation for a particular TI Resource.

You are authorized to use, copy and modify any individual TI Resource only in connection with the development of applications that include the TI product(s) identified in such TI Resource. NO OTHER LICENSE, EXPRESS OR IMPLIED, BY ESTOPPEL OR OTHERWISE TO ANY OTHER TI INTELLECTUAL PROPERTY RIGHT, AND NO LICENSE TO ANY TECHNOLOGY OR INTELLECTUAL PROPERTY RIGHT OF TI OR ANY THIRD PARTY IS GRANTED HEREIN, including but not limited to any patent right, copyright, mask work right, or other intellectual property right relating to any combination, machine, or process in which TI products or services are used. Information regarding or referencing third-party products or services does not constitute a license to use such products or services, or a warranty or endorsement thereof. Use of TI Resources may require a license from a third party under the patents or other intellectual property of the third party, or a license from TI under the patents or other intellectual property of TI.

TI RESOURCES ARE PROVIDED "AS IS" AND WITH ALL FAULTS. TI DISCLAIMS ALL OTHER WARRANTIES OR REPRESENTATIONS, EXPRESS OR IMPLIED, REGARDING TI RESOURCES OR USE THEREOF, INCLUDING BUT NOT LIMITED TO ACCURACY OR COMPLETENESS, TITLE, ANY EPIDEMIC FAILURE WARRANTY AND ANY IMPLIED WARRANTIES OF MERCHANTABILITY, FITNESS FOR A PARTICULAR PURPOSE, AND NON-INFRINGEMENT OF ANY THIRD PARTY INTELLECTUAL PROPERTY RIGHTS.

TI SHALL NOT BE LIABLE FOR AND SHALL NOT DEFEND OR INDEMNIFY YOU AGAINST ANY CLAIM, INCLUDING BUT NOT LIMITED TO ANY INFRINGEMENT CLAIM THAT RELATES TO OR IS BASED ON ANY COMBINATION OF PRODUCTS EVEN IF DESCRIBED IN TI RESOURCES OR OTHERWISE. IN NO EVENT SHALL TI BE LIABLE FOR ANY ACTUAL, DIRECT, SPECIAL, COLLATERAL, INDIRECT, PUNITIVE, INCIDENTAL, CONSEQUENTIAL OR EXEMPLARY DAMAGES IN CONNECTION WITH OR ARISING OUT OF TI RESOURCES OR USE THEREOF, AND REGARDLESS OF WHETHER TI HAS BEEN ADVISED OF THE POSSIBILITY OF SUCH DAMAGES.

You agree to fully indemnify TI and its representatives against any damages, costs, losses, and/or liabilities arising out of your non-compliance with the terms and provisions of this Notice.

This Notice applies to TI Resources. Additional terms apply to the use and purchase of certain types of materials, TI products and services. These include; without limitation, TI's standard terms for semiconductor products http://www.ti.com/sc/docs/stdterms.htm), evaluation modules, and samples (http://www.ti.com/sc/docs/sampterms.htm).

Mailing Address: Texas Instruments, Post Office Box 655303, Dallas, Texas 75265